Applied Catalysis A: General 485 (2014) 188–195

Contents lists available at ScienceDirect

Applied Catalysis A: General

journal homepage: www.elsevier.com/locate/apcata

Anatase TiO_2 nanoparticles–carbon nanotubes composite: Optimization synthesis and the relationship of photocatalytic degradation activity of acyclovir in water

Jiangyao Chen[a], Haiying Luo[a,b], Huixian Shi[a], Guiying Li[a], Taicheng An[a,*]

[a] State Key Laboratory of Organic Geochemistry and Guangdong Key Laboratory of Environmental Resources Utilization and Protection, Guangzhou Institute of Geochemistry, Chinese Academy of Sciences, Guangzhou 510640, China
[b] University of Chinese Academy of Sciences, Beijing 100049, China

ARTICLE INFO

Article history:
Received 18 April 2014
Received in revised form 4 August 2014
Accepted 5 August 2014
Available online 13 August 2014

Keywords:
MWCNTs based composite photocatalyst
Optimization synthesis
Center composite design
Photocatalytic activity
Antiviral pharmaceuticals

ABSTRACT

In this study, TiO_2 nanoparticles–multi-walled carbon nanotubes (TNPs–MWCNTs) composite photocatalyst was prepared via a simple soft-template hydrothermal method and optimized based on the center composite design (CCD). Four synthesis parameters, including amount of Pluronic P123, MWCNTs, and tetrabutyl titanate (TBT) as well as hydrothermal temperature, were selected to investigate their effects on the photocatalytic activity of the resultant composites toward acyclovir in water. Results showed that the most important parameter to prepare TNPs–MWCNTs composite with high photocatalytic activity is hydrothermal temperature, followed by the amount of MWCNTs, while the amount of TBT and P123 played relatively less important roles in this work. Based on the theoretical and experimental results, the highest photocatalytic degradation efficiency of acyclovir was up to 98.6% using the TNPs–MWCNTs composite photocatalyst synthesized under the optimum parameters, 240 °C of hydrothermal temperature, 0.06 g of MWCNTs, 1.10 g of TBT, and 0.10 g of P123. All these results demonstrate that the CCD method can be efficiently applied in the optimization synthesis of composite photocatalysts with high performance for environmental remediation.

1. Introduction

Since the first detection in the environment decades ago, the occurrence and fate of pharmaceuticals in aquatic environments have gained significant attention due to their adverse health effects, such as aquatic toxicity, genotoxicity and endocrine disruption [1–3]. As a class of pharmaceuticals, antiviral pharmaceuticals used for the treatment of influenza, herpes or hepatitis for humans and animals have recently been widely detected in the environment [4,5]. Some of them can be easily degraded, but others persist for a long time and accumulate in various organs of humans and animals, which are harmful to ecological species and humans [6]. Therefore, various technologies have been applied to remove antiviral pharmaceuticals from environment, such as adsorption, incineration, biological degradation, etc. [7], while heterogeneous photocatalysis has been proven to be a promising and efficient technology for this purpose [8]. During the photocatalytic process, the most important parameter is the photocatalyst, among which TiO_2 has been frequently used for the degradation of pharmaceuticals [9–13]. However, the concentration of antiviral pharmaceuticals in water environments are generally extremely low [14], thus the small surface area of TiO_2 results in its low adsorption capability and then low photocatalytic efficiency to them [15,16]. Moreover, small particle size of most TiO_2 arises the problem in the catalyst-recovering stage and hinders its effectively commercial applications [17,18]. Therefore, it is urgent to develop TiO_2-based catalysts possessing high active surface area, together with better recovery properties to enhance the photocatalytic degradation efficiency of antiviral pharmaceuticals.

Currently, TiO_2 supported on multi-walled carbon nanotubes (MWCNTs) have attracted much attention, since the combination of MWCNTs with TiO_2 is found to greatly improve the photocatalytic activity of TiO_2 [19–26]. In these composites, MWCNTs can not only act as an electron reservoir to suppress the recombination of photogenerated electron–hole pairs, but also act as a excellent adsorbent for organic pollutants owing to their hollow and layered structures with large specific surface area, which can subsequently enhance

* Corresponding author. Tel.: +86 20 85291501; fax: +86 20 85290706.
E-mail address: antc99@gig.ac.cn (T. An).

http://dx.doi.org/10.1016/j.apcata.2014.08.004
0926-860X/

the photocatalytic activity of TiO_2. Unfortunately, all these reported works invariably applied the approach of single-variable-at-a-time (SVAT) to synthesize the TiO_2–MWCNTs composites, although previous publication has proved that SVAT approach possesses lots of drawbacks, such as time-consuming and the absence of interactions between different variables as well as the inefficiency to predict the true optimum [8]. To overcome these shortcomings of SVAT method, central composite design (CCD) method was used as an alternative method to design and optimize the synthesis of photocatalyst [27]. It is because the interactions of possible influencing factors on the desired responses can be evaluated with CCD method just by using minimum number of designed experiments, and then an optimal reaction condition can be much more easily accomplished. Further, for the synthesis of TiO_2–MWCNTs composite, the hydrothermal methods with different parameters have been reported [28–30]. Among all these parameters, hydrothermal temperature and amount of MWCNTs are found to be two very significant parameters during the synthesis process, which play more important roles than other selected parameters to influence the photocatalytic activity of the resultant TiO_2–MWCNTs composites in our previous work [31].

Therefore, to further verify the important roles of these two parameters in the hydrothermal synthesis of TiO_2–MWCNTs composite, in this study, hydrothermal temperature and amount of MWCNTs with other two key parameters (amount of Pluronic P123 and tetrabutyl titanate (TBT)) were selected to design and optimize the synthesis of TiO_2 nanoparticles–MWCNTs (TNPs–MWCNTs) composite photocatalysts with CCD method. Acyclovir, a typical antivirus pharmaceutical, was chosen as a model pollutant to evaluate the photocatalytic activity of the resultant composite photocatalysts. It should be noted that this is the first time to investigate the photocatalytic degradation of antivirus pharmaceuticals on TiO_2–MWCNTs composite photocatalyst. Furthermore, the desired response values (the degradation efficiency of acyclovir) predicted using CCD was compared with the experimental photocatalytic degradation efficiencies of acyclovir. In addition, the relationship between the photocatalytic activity of the prepared TNPs–MWCNTs composite photocatalysts for the degradation of acyclovir and the synthesis parameters was also attempted based on the experimental results.

2. Experimental

2.1. Design, synthesis and characterization of photocatalysts

The chemometric approach, CCD, was applied to design the photocatalyst, and the analysis of the experimental data was supported by the Design-Expert software (trail version 8, Stat-Ease, Inc., MN, USA). Four independent variables (amount of P123, amount of MWCNTs, amount of TBT and hydrothermal temperature) were selected to investigate their effects on the synthesis of TNPs–MWCNTs composite photocatalysts, and the photocatalytic degradation efficiency of acyclovir in water was selected as the response. The four chosen variables were converted to dimensionless ones (A, B, C, D), with the coded values at levels: −2, −1, 0, +1, +2 and the determined values of the variables are presented in Table S1. It can be seen that the five levels for controlling factors are in the range of 0.10–2.50 g, 0.01–0.09 g, 0.10–1.10 g, and 100–240 °C for the factors *A*, *B*, *C* and *D*, respectively. The complete experimental design matrix and the responses are also shown in Table 1.

For synthesis of TNPs–MWCNTs composite photocatalysts, MWCNTs (Shenzhen Nanotech Port Co., Ltd., China) was firstly purified according to the procedure in our previous work [31]. Then, designed amounts of P123, purified MWCNTs and TBT were mixed with 20% (V/V) acetic acid solution and stirring for 60 min. The mixtures were transformed into Teflon-line autoclave with a volume of 100 mL and kept at selected hydrothermal temperature for 72 h. After reaction, the products were obtained by centrifuge, washed with distilled water, dried at 80 °C and finally calcined under 400 °C for 1 h. The composite photocatalysts were then characterized by X-ray diffractometer (XRD, Rigaku Dmax X-ray diffractometer), UV–visible spectrophotometer (UV-vis, UV-2501PC) and Scanning electron microscopy (SEM, Quanta 400F).

Table 1
Experimental design matrix and the value of responses based on experiment run.

Run	Independent variables				Degradation efficiency (%)	
	A	*B*	*C*	*D*	Experimental	Predicted
1	1.30	0.09	0.60	170	31.7	50.0
2	1.30	0.05	0.60	170	59.6	60.6
3	1.90	0.03	0.35	205	94.1	89.7
4	0.10	0.05	0.60	170	47.1	60.4
5	0.70	0.07	0.35	205	59.1	58.6
6	0.70	0.03	0.35	205	88.8	83.3
7	1.90	0.03	0.35	135	65.3	68.9
8	1.30	0.05	0.10	170	36.3	50.9
9	0.70	0.07	0.35	135	36.4	18.8
10	1.30	0.05	1.10	170	65.0	64.6
11	1.90	0.07	0.35	135	49.2	36.0
12	1.30	0.05	0.60	170	64.1	60.6
13	0.70	0.07	0.85	205	83.0	76.4
14	1.30	0.05	0.60	170	58.7	60.6
15	1.30	0.05	0.60	100	23.4	40.2
16	1.30	0.01	0.60	170	87.9	83.9
17	0.70	0.03	0.35	135	58.9	54.7
18	0.70	0.03	0.85	205	75.6	77.4
19	2.50	0.05	0.60	170	69.0	70.0
20	1.30	0.05	0.60	170	60.1	60.6
21	1.90	0.03	0.85	135	75.6	64.7
22	1.30	0.05	0.60	240	87.5	85.0
23	1.90	0.07	0.85	135	52.9	55.5
24	1.90	0.03	0.85	205	55.1	69.8
25	0.70	0.07	0.85	135	59.2	52.3
26	0.70	0.03	0.85	135	65.7	64.5
27	1.90	0.07	0.35	205	69.6	67.9
28	1.90	0.07	0.85	205	78.9	71.8

2.2. Photocatalytic activity evaluation

The photocatalytic activities of the prepared TNPs–MWCNTs composite photocatalysts were tested by the degradation of acyclovir in water. The photocatalytic reactor consists of a 160 mL Pyrex glass bottle with a jacket outside and a 125 W high pressure Hg lamp in parallel to the Pyrex glass bottle. In a typical reaction process, 20 mg of the prepared composite photocatalyst was mixed with 50 mL acyclovir solution with the initial concentration of 10 mg L^{-1}. Before switching on the lamp with a maximum emitting radiation of 365 nm (GGZ125, Shanghai Yaming Lighting Co., Ltd., the UV intensity was controlled at 1.17 mW cm^{-2}, which was measured by an UV RADIOMETER from Photoelectric Instrument Factory of Beijing Normal University located in the middle of the reactor which was parallel to the lamp), 30 min dark adsorption was allowed in a quartz tube reactor with a jacket outside to ensure the establishment of adsorption–desorption equilibrium. Stirring was kept during the photocatalytic process without air-purging. The concentrations of acyclovir after 210 min degradation were determined by Ultra Performance Liquid Chromatography (UPLC) with an Acquity UPLC HSS T3 (1.8 μm, 100 mm × 2.1 mm) column at wavelength 252 nm. The mobile phase was a mixture of KH_2PO_4 solution and acetonitrile (V:V = 9:1) at the flow rate of 0.3 mL min^{-1}.

The photocatalytic degradation efficiency was calculated according to the Eq. (1).

$$\text{Degradation efficiency } (\%) = \frac{C}{C_0} \times 100\% \quad (1)$$

where C presented the content of residual pollutant and C_0 was its original content.

3. Results and discussion

3.1. Establishment and analysis of model

According to the Design-Expert software, a semi-empirical expression which is consisted of 15 statistically significant coefficients is obtained and expressed as follows:

$$Y = 60.63 + 2.40A - 8.48B + 3.42C + 11.22D + 0.74AB - 3.51AC - 1.96AD + 5.93BC + 2.80BD - 3.92CD + 1.14A^2 + 1.58B^2 - 0.71C^2 + 0.49D^2 \quad (2)$$

where Y is the response variable of degradation efficiency of acyclovir. The A, B, C and D represent four experimental factors, respectively.

Eq. (2) can be used to predict the photocatalytic degradation efficiency of prepared TNPs–MWCNTs composites toward acyclovir, and the correspondingly experimental and predicted data are shown in Table 1. Clearly, the predicted values from the model are very close to the experimental ones, which can be further evidenced by plotting the predicted photocatalytic values against the experimental values as shown in Fig. S1, where the line of the best fit with the slope of 0.7545 and $R^2 = 0.7545$ are obtained. Moreover, as variance can be used to evaluate the significance and the adequacy of the model [32,33], the analysis of variance of the quadratic model is displayed in Table S2. If the model is adequacy, F-value should be greater than the tabulated value of F-distribution for a certain number of degrees of freedom in the model at a level of significance [34]. Obviously from the table, the F-value for regression of the degradation model is 2.85, which is greater than the value of $F_{(14,\,13)}$ (2.55) at 95% significance, indicating the adequacy of the model. Moreover, the P value (significant probability values, 0.0335) is smaller than 0.05, suggesting the significance of the model. Besides correlation coefficient and variance, the residuals are also applied to evaluate the adequacy of the model, and Fig. S2 displays the internally studentized residual plot. It can be seen that all residuals are well distributed along the straight line (Fig. S2a), indicating that there is no severe non-normality and the residuals are distributed between −3 and +3 without any systematic structure and obvious pattern no matter how the predicted value varies, indicating that the residuals appear to be a random scatter (Fig. S2b). From these results, it can be concluded that the model obtained is adequate to describe the relationship between the degradation efficiency and the synthesis parameters to prepare TNPs–MWCNTs composites.

To find out the importance of the each factor in Eq. (2), the Pareto analysis is used to calculate the percentage of each variable on the response according to the Eq. (3) [35]:

$$P_i = \left(\frac{a_i^2}{\sum a_i^2}\right) \times 100 \quad (i \neq 0) \quad (3)$$

where P_i represents the percentage effect of each variable and a_i represents statistically significant coefficients in Eq. (2), respectively.

Fig. 1 shows the corresponding results of the Pareto graphic analysis. Clearly, the most important parameter to prepare TNPs–MWCNTs composite photocatalysts with high degradation efficiency is hydrothermal temperature (D, 42.7%), followed by the amount of MWCNTs (B, 24.4%), while the amount of TBT (C, 4.0%) and P123 (A, 2.0%) play less important roles in this work. Moreover, the degradation efficiency is also affected by the interrelated variables such as two factor interactions (BC, 11.9%). Interestingly,

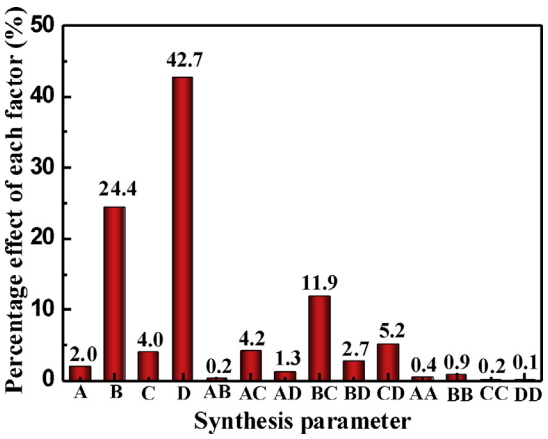

Fig. 1. Pareto graphic analysis for the degradation efficiency of acyclovir using TNPs–MWCNTs composite as photocatalysts.

this result is very consistent with that reported in our previous work that hydrothermal temperature and amount of MWCNTs are more important parameters for the hydrothermal preparation of TiO_2–MWCNTs composite photocatalysts with high degradation efficiency to gaseous styrene, although other two parameters are varied and more complicated synthesis procedure is used here [31]. All these results suggest that hydrothermal temperature and amount of MWCNTs should be considered preferential in the case of hydrothermal synthesis of MWCNTs based composite photocatalyst.

3.2. Analysis of contour and response surface plots

The two-dimensional contour and three-dimensional response surface plots are constructed by using the statistical software to illustrate the interaction effects of selected factors on the degradation efficiency and finally find out the optimal parameters to synthesize TNPs–MWCNTs composite photocatalyst with the highest degradation efficiency of acyclovir, as shown in Fig. 2. Moreover, to establish the relationship between the synthesis parameters and the degradation efficiency, the XRD patterns, UV–vis absorption spectra and SEM images of some typically prepared TNPs–MWCNTs composite photocatalysts are also displayed in Figs. 3–8.

Since the Pareto graphic analysis results reveal that hydrothermal temperature is the most important parameter for the preparation of TNPs–MWCNTs composite photocatalysts with high degradation efficiency, the interaction effects of three combinations for the synthesis parameters (hydrothermal temperature with amount of P123, hydrothermal temperature with amount of MWCNTs, and hydrothermal temperature with amount of TBT) on the degradation efficiency of resultant composite photocatalysts are correspondingly investigated. Fig. 2a shows the effect of hydrothermal temperature and amount of P123 on the degradation efficiency of acyclovir (0.05 g MWCNTs; 0.60 g TBT). Clearly, when the hydrothermal temperature is fixed at 170 °C with the amount of P123 increasing from 0.10 to 2.50 g, the degradation efficiencies continuously increases from 47.1% to 69.0%, indicating that the higher amount of P123 added in the reaction is, the higher photocatalytic activity of the resultant composite is. Reasonable explanation can be ascribed from the characteristic results. As shown in Figs. 3a, 4a and 5, all samples show similar and typical XRD patterns of anatase TiO_2 (Fig. 3a), where characteristic diffraction peaks of the XRD patterns for all samples at $2\theta = 25.3°$, 37.8°, 48.0°, 54.0°, 55.3°, 62.4°, and 68.7° are attributed to the {1 0 1}, {0 0 4}, {2 0 0}, {1 0 5}, {2 1 1}, {2 0 4}, and {1 1 2} planes of anatase TiO_2. However, their morphological and optical properties are different. With the increase of the amount of P123 from 0.10 to 2.50 g, the

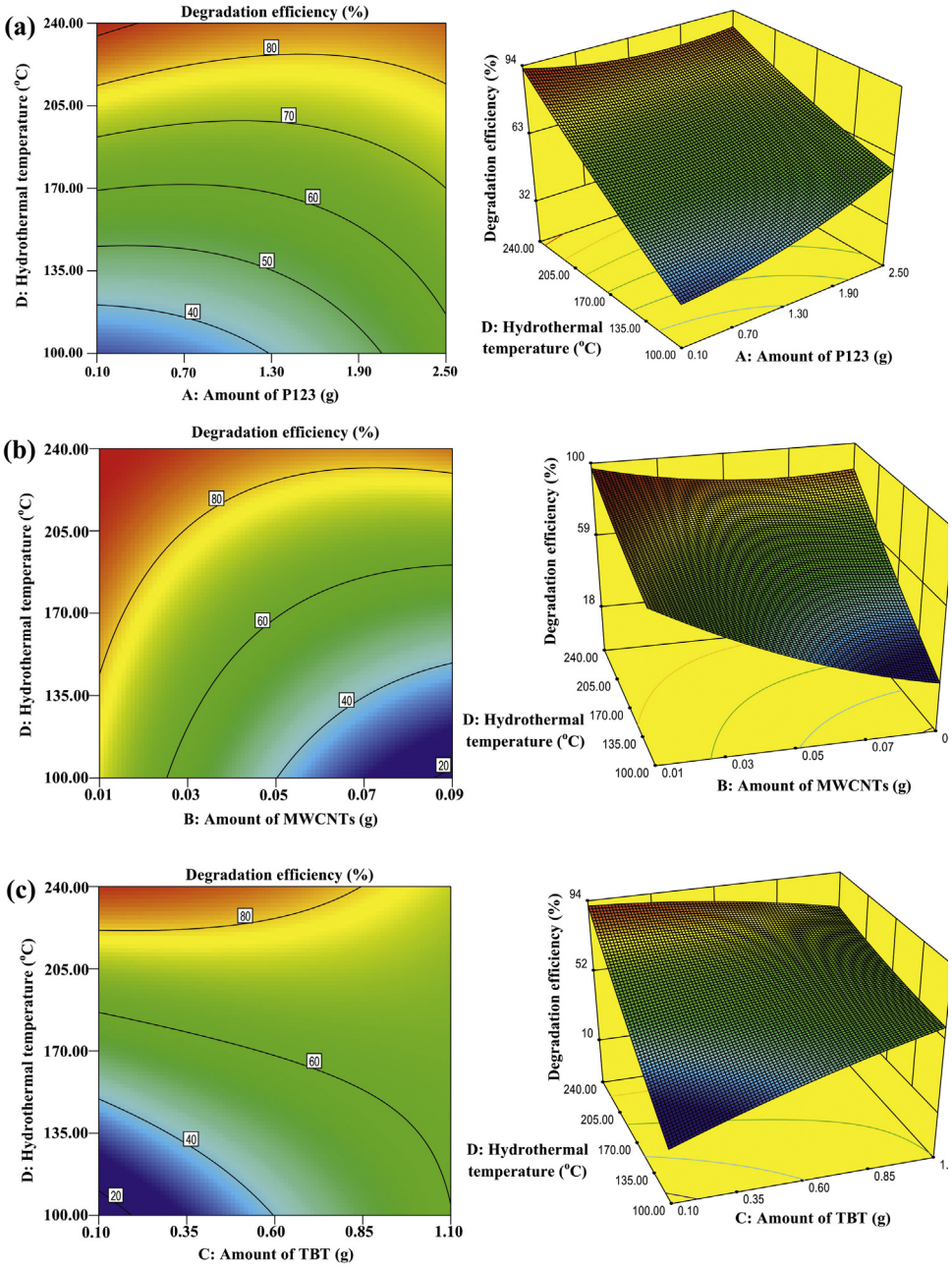

Fig. 2. The contour and response surface plots of degradation efficiency of acyclovir by TNPs–MWCNTs composite photocatalysts as the function of hydrothermal temperature with amount of P123 (a), MWCNTs (b) and TBT (c).

UV absorption intensity of the resultant TNPs–MWCNTs is continuously and greatly enhanced (Fig. 4a), which can be contributed to the smaller-sized and better-dispersed TiO_2 nanoparticles in the composite (Fig. 5). The reason is that compared with agglomerated TiO_2 particles in the bulk material of blank-TiO_2, the large specific area of small-sized TiO_2 particles ensures efficient UV light absorption and provides more photoreactive sites for degradation reaction [36]. In the case of hydrothermal temperature, the degradation efficiency is found to greatly increase from 23.4% to 87.5% with the increase of the hydrothermal temperature from 100 to 240 °C. The correspondingly structural, optical and morphological properties of the resultant composite photocatalysts are displayed in Figs. 3d, 4d and 6. Apparently, the characteristic peaks of XRD patterns of the composites become much stronger as the hydrothermal temperature increases (Fig. 3d), indicating the enhancement of the crystallinity, which can reduce the electron and hole recombination and then lead to higher photocatalytic activity [37]. This result can also be verified from the SEM images (Fig. 6). That is, TiO_2 nanoparticles with more regular morphology and uniform size in the resultant composite can be observed, which are more closely contacted with MWCNTs as the increase of the hydrothermal temperature. The tighter connect between TiO_2 nanoparticles and MWCNTs can more efficiently accelerate the transfer of the photo-electron from TiO_2 to MWCNTs, suppress the recombination of photo-electron and photo-hole pairs, as well as improve the photocatalytic activity. On the other hand, no significant change of UV absorption intensity is found with increasing the hydrothermal temperature (Fig. 4d), implying negligible impact of hydrothermal temperature to the UV absorption ability of the resultant composites. Therefore, the highest degradation efficiency is

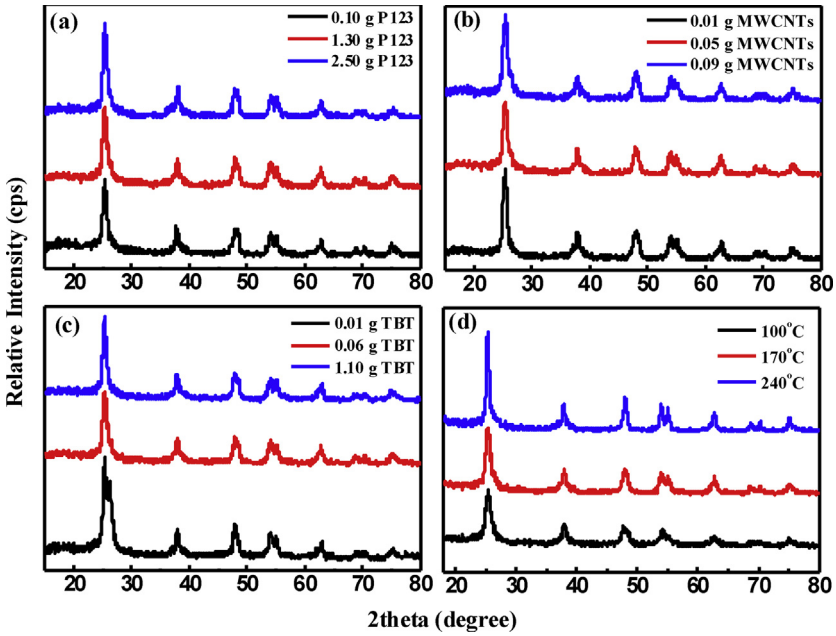

Fig. 3. XRD patterns of composite photocatalysts prepared with different (a) amount of P123 (MWCNTs: 0.05 g; TBT: 0.60 g; hydrothermal temperature: 170 °C); (b) amount of MWCNTs (P123: 1.30 g; TBT: 0.60 g; hydrothermal temperature: 170 °C); (c) amount of TBT (P123: 1.30 g; MWCNTs: 0.05 g; hydrothermal temperature: 170 °C); (d) hydrothermal temperature (P123: 1.30 g, MWCNTs: 0.05 g; TBT: 0.60 g).

obtained for the TNPs–MWCNTs composite prepared with a highest amount of P123 addition (2.50 g) and maximum hydrothermal temperature (240 °C).

It should be mentioned herewith that, compared with our previous results [31], completely different trends are observed for the influence of hydrothermal temperature to the photocatalytic activity of the resultant TiO_2–MWCNTs composites. That is, the increase of the hydrothermal temperature leads to the increase of the photocatalytic activity of resultant composite photocatalysts in this study, but decrease of that was found in our previous work [31]. The possible reason may be ascribed to the different structure properties of the resultant TiO_2–MWCNTs composite photocatalysts. In previous work, the TiO_2 particle size played the most important role in the influence of the UV absorption intensity of the resultant composite and then their photocatalytic activity. That is, the average diameter of the TiO_2 particles in the composite photocatalysts greatly increased from submicron to micro size with the continuous increase of the hydrothermal temperature, leading to the continuous decrease of the UV absorption intensity and then of the degradation efficiency. However, in this study, with the increase of the hydrothermal temperature, TiO_2 nanoparticles with similar size are formed in the resultant composites with no

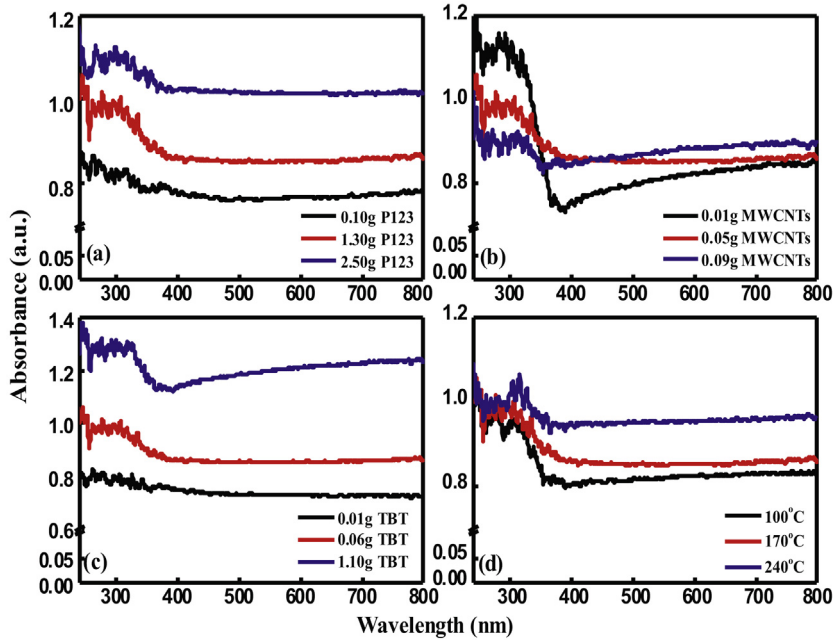

Fig. 4. UV–vis absorption spectra of composite photocatalysts prepared with different (a) amount of P123 (MWCNTs: 0.05 g; TBT: 0.60 g; hydrothermal temperature: 170 °C); (b) amount of MWCNTs (P123: 1.30 g; TBT: 0.60 g; hydrothermal temperature: 170 °C) (c) amount of TBT (P123: 1.30 g; MWCNTs: 0.05 g; hydrothermal temperature: 170 °C); (d) hydrothermal temperature (P123: 1.30 g, MWCNTs: 0.05 g; TBT: 0.60 g).

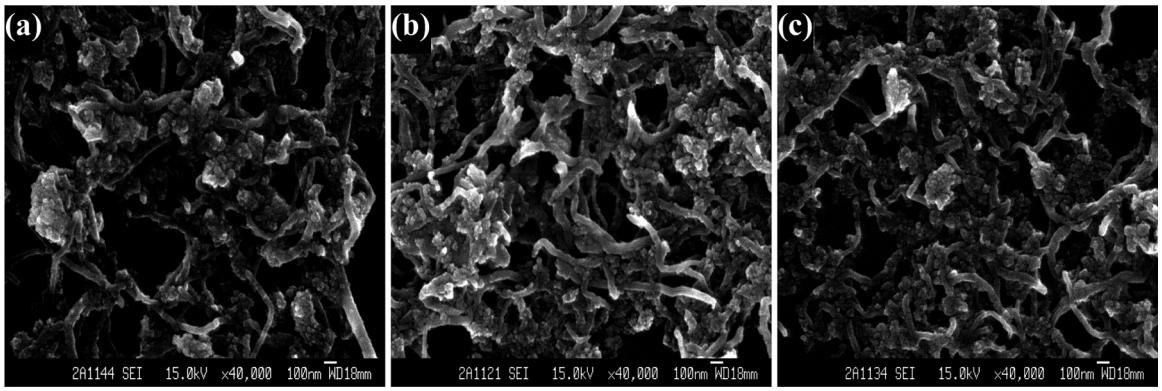

Fig. 5. SEM images of composite photocatalysts prepared with 0.05 g MWCNTs, 0.60 g TBT, hydrothermal temperature of 170 °C, and (a) 0.10 g; (b) 1.30 g; (c) 2.50 g P123.

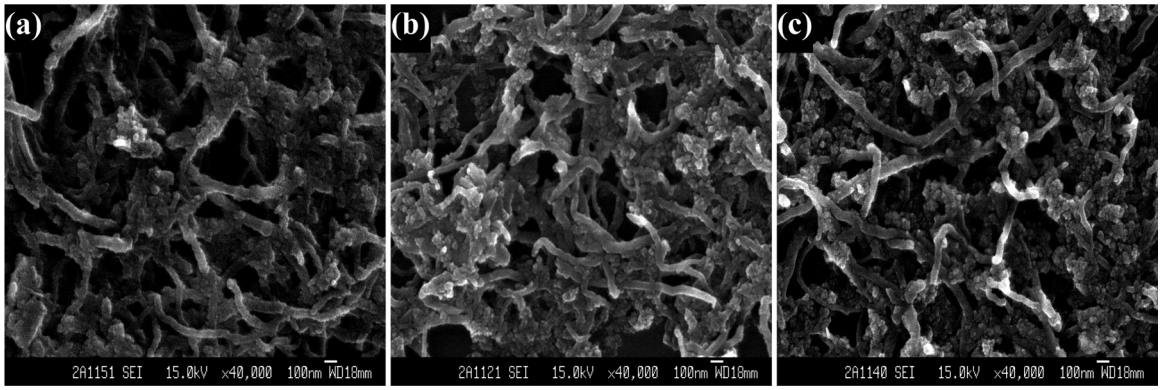

Fig. 6. SEM images of composite photocatalysts prepared with 1.30 g P123, 0.05 g MWCNTs, 0.60 g TBT and hydrothermal temperature of (a) 100 °C; (b) 170 °C; (c) 240 °C.

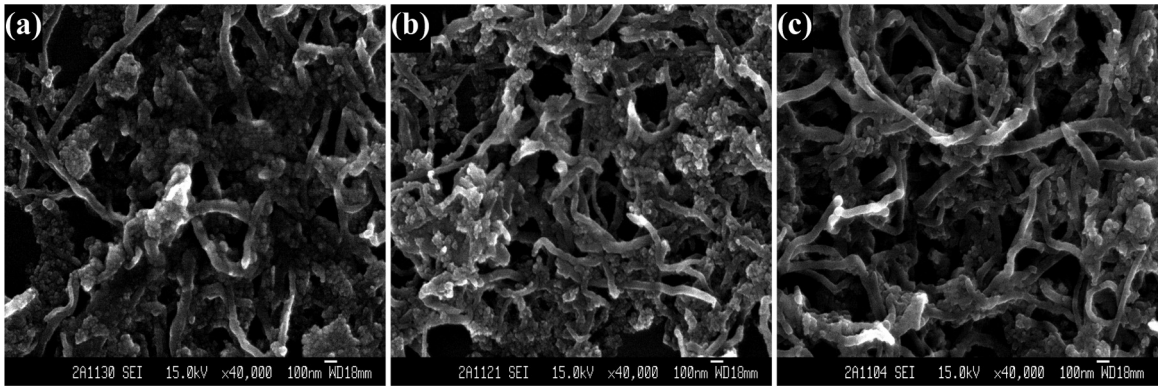

Fig. 7. SEM images of composite photocatalysts prepared with 1.30 g P123, 0.60 g TBT, hydrothermal temperature of 170 °C and (a) 0.01 g; (b) 0.05 g; (c) 0.09 g MWCNTs.

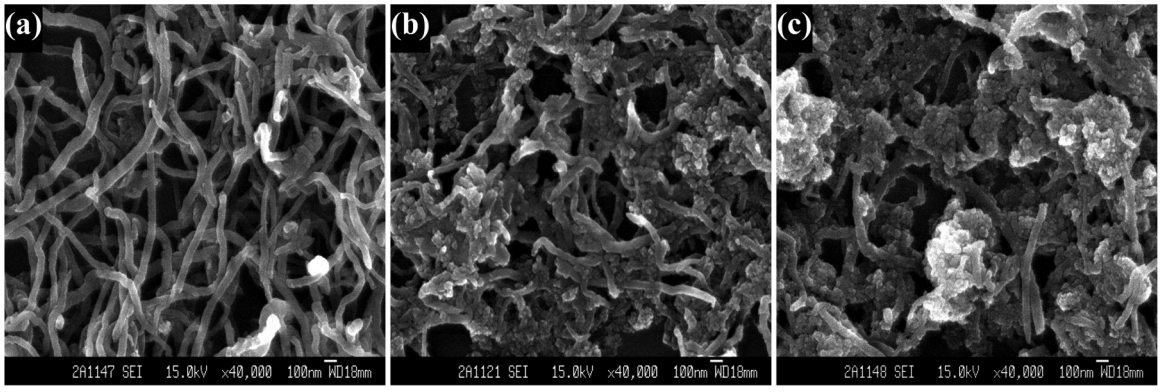

Fig. 8. SEM images of composite photocatalysts prepared with 1.30 g P123, 0.05 g MWCNTs, hydrothermal temperature of 170 °C and (a) 0.10 g; (b) 0.60 g; (c) 1.10 g TBT.

significant change of UV absorption intensity, while the enhancement of the crystallinity of the resultant composites can be found. Then, the increase of the degradation efficiency in this study is dominantly due to the enhancement of the crystallinity. In one word, higher hydrothermal temperature is preferred in this study to obtain composites with higher crystallinity and then with higher photocatalytic activity.

Furthermore, the effect of hydrothermal temperature and amount of MWCNTs on the degradation efficiency of acyclovir are also investigated when the amounts of P123 and TBT are fixed at 1.30 and 0.60 g, respectively (Fig. 2b). Obviously, the degradation efficiencies decrease dramatically from 87.9% to 31.7% with increase of the amount of MWCNTs from 0.01 to 0.09 g, indicating the higher amount of MWCNTs added, the worse photocatalytic activity of the resultant composite obtained. The corresponding characteristic results are shown in Figs. 3b, 4b and 7. When 0.01 g MWCNTs is added into the preparation recipe, only peaks of anatase TiO_2 can be observed form the resultant composite due to low content of MWCNTs unable to be detected by XRD (Fig. 3b). With increasing the amount of MWCNTs to 0.05 and 0.09 g, a peak at $2\theta = 26.0^\circ$ for MWCNTs can be more and more clearly observed. Moreover, fewer and fewer TiO_2 particles can be observed when more and more MWCNTs are added (Fig. 7b and c), leading to the continuously decrease of the absorption intensity in the UV region (Fig. 4b), and thus resulting in the decrease of the degradation efficiency. As well known, the adsorption of pollutants onto the photocatalyst surface is the first step of photocatalytic reaction [15], and the addition of MWCNTs can enhance the adsorption and enrichment capacity of the composite photocatalyst to organics [19,38]. In this study, a small amount of MWCNTs (0.01 g) is enough to obtain the composite with high adsorption capacity to show more positive synergetic effect (such as higher UV light absorption) to the photocatalytic activity than that with higher content of MWCNTs.

To investigate the interaction effect of hydrothermal temperature and amount of TBT on the photocatalytic degradation efficiency of acyclovir, the degradation experiments are conducted using TNPs–MWCNTs composite photocatalysts prepared with different amount of TBT and hydrothermal temperature varying from 0.10 to 1.10 g and 100 to 240 °C, respectively, at constant amounts of P123 (1.30 g) and MWCNTs (0.05 g). As shown in Fig. 2c, similar to the results obtained above, the highest degradation efficiency is achieved when the hydrothermal temperature is maintained at its maximum (240 °C). In the case of amount of TBT, there is a continuously increase in the degradation efficiency from 36.3% to 65.0% with increasing the amount of TBT from 0.10 to 1.10 g. From the results of XRD patterns and SEM images of the TNPs–MWCNTs composite photocatalysts, it is clear to see that the intensity of diffraction peak at $2\theta = 26.0^\circ$ for MWCNTs is rapidly weakened (Fig. 3c), while more TiO_2 nanoparticles can be observed in the composites with the increase of the added amount of TBT from 0.10 to 1.10 g (Fig. 8a and c), leading to the obvious increase of the absorption intensity in the UV region (Fig. 4c). This might be attributed to the electron transfer of TiO_2 from the valence band to conduction band [39]. All these confirm that the composite photocatalyst prepared with higher added amount of TBT possesses higher photocatalytic activity in this work.

Overall, the final objective of the optimization is to simply and effectively obtain the optimum synthesis parameters for the preparation of TNPs–MWCNTs composite photocatalyst with highest photocatalytic degradation efficiency of acyclovir based on the experimental results. Herein, by using a numerical optimization method in the Design Expert software, the desired goals for all the variables are chosen in the experimental range that the amount of P123, MWCNTs, and TBT as well as hydrothermal temperature are in the range of 0.10–2.50 g, 0.01–0.09 g, 0.10–1.10 g and 100–240 °C, respectively, while the degradation efficiency is defined as "maximize" with the upper limit of 100% (the theoretical high). Then, the optimum values of the variables to synthesize TNPs–MWCNTs composite photocatalyst with the highest degradation efficiency of acyclovir (98.6%) are 240 °C of hydrothermal temperature, 0.06 g of MWCNTs, 1.10 g of TBT and 0.10 g of P123, respectively, as shown in Fig. S3.

4. Conclusions

In this study, the CCD method was applied to optimize the synthesis of TNPs–MWCNTs composite photocatalyst with the highest photocatalytic degradation efficiency of acyclovir in water. Among the synthesis parameters in the experimental design, the hydrothermal temperature was expected playing the most important role in the photocatalytic degradation activity of acyclovir. Higher hydrothermal temperature was beneficial for synthesizing the TNPs–MWCNTs composite with higher degradation efficiency. Meanwhile, other three synthesis parameters, such as amounts of MWCNTs, TBT and P123 also showed the influence on the degradation performance of the composite photocatalysts. The worse photocatalytic degradation efficiency of acyclovir was obtained when the composite photocatalysts were prepared under these parameters with lowest or highest values. Finally, the optimal values of synthesis parameters were obtained as 240 °C, 0.06 g, 1.10 g and 0.10 g for hydrothermal temperature, amount of MWCNTs, amount of TBT and amount of P123, respectively, based on the experimental data.

Acknowledgements

This is contribution No. 1926 from GIGCAS. The authors appreciate the financial supports from NSFC (41373102 and 40973068), Team Project from Natural Science Foundation of Guangdong Province, China (S2012030006604), Science and Technology Project of Guangdong Province, China (2012A032300010) and earmarked Fund of SKLOG (SKLOG2011A02).

Appendix A. Supplementary data

Supplementary data associated with this article can be found, in the online version, at http://dx.doi.org/10.1016/j.apcata.2014.08.004.

References

[1] C.J. Lin, W.T. Yang, Chem. Eng. J. 237 (2014) 131–137.
[2] H. Yang, G.Y. Li, T.C. An, Y.P. Gao, J.M. Fu, Catal. Today 153 (2010) 200–207.
[3] T.C. An, H. Yang, W.H. Song, G.Y. Li, H.Y. Luo, W.J. Cooper, J. Phys. Chem. A 114 (2010) 2569–2575.
[4] C. Prasse, M. Wagner, R. Schulz, T.A. Ternes, Environ. Sci. Technol. 46 (2012) 2169–2178.
[5] G.C. Ghosh, N. Nakada, N. Yamashita, H. Tanaka, Environ. Health Perspect. 118 (2010) 103–107.
[6] X. Nie, J.Y. Chen, G.Y. Li, H.X. Shi, H.J. Zhao, P.K. Wong, T.C. An, J. Chem. Technol. Biotechnol. 88 (2013) 1488–1497.
[7] S. Jain, P. Kumar, R.K. Vyas, P. Pandit, A.K. Dalai, Water Air Soil Pollut. 224 (2013) 1410–1428.
[8] T.C. An, J.B. An, H. Yang, G.Y. Li, H.X. Feng, X.P. Nie, J. Hazard. Mater. 197 (2011) 229–236.
[9] S. Murphy, C. Saurel, A. Morrissey, J. Tobin, M. Oelgemoller, K. Nolan, Appl. Catal. B: Environ. 119 (2012) 156–165.
[10] A.M. Hu, X. Zhang, K.D. Oakes, P. Peng, Y.N. Zhou, M.R. Servos, J. Hazard. Mater. 189 (2011) 278–285.
[11] T.C. An, H. Yang, G.Y. Li, W.H. Song, W.J. Cooper, X.P. Nie, Appl. Catal. B: Environ. 94 (2010) 288–294.
[12] H. Yang, T.C. An, G.Y. Li, W.H. Song, W.J. Cooper, H.Y. Luo, X.D. Guo, J. Hazard. Mater. 179 (2010) 834–839.
[13] H.S. Fang, Y.P. Gao, G.Y. Li, J.B. An, P.K. Wong, H.Y. Fu, S.D. Yao, X.P. Nie, T.C. An, Environ. Sci. Technol. 47 (2013) 2704–2712.
[14] C. Prasse, M.P. Schlusener, R. Schulz, T.A. Ternes, Environ. Sci. Technol. 44 (2010) 1728–1735.

[15] J.Y. Chen, G.Y. Li, Z.G. He, T.C. An, J. Hazard. Mater. 190 (2011) 416–423.
[16] Z.M. Sun, C.H. Bai, S.L. Zheng, X.P. Yang, R.L. Frost, Appl. Catal. A: Gen. 458 (2013) 103–110.
[17] R. van Grieken, J. Aguado, M.J. Lopez-Munoz, J. Marugan, J. Photochem. Photobiol. A 148 (2002) 315–322.
[18] T.J. Xin, M.L. Ma, H.P. Zhang, J.W. Gu, S.J. Wang, M.J. Liu, Q.Y. Zhang, Appl. Surf. Sci. 288 (2014) 51–59.
[19] T.C. An, J.Y. Chen, X. Nie, G.Y. Li, H.M. Zhang, X.L. Liu, H.J. Zhao, ACS Appl. Mater. Interfaces 4 (2012) 5988–5996.
[20] S. Wang, L.J. Ji, B. Wu, Q.M. Gong, Y.F. Zhu, J. Liang, Appl. Surf. Sci. 255 (2008) 3263–3266.
[21] B. Gao, G.Z. Chen, G.L. Puma, Appl. Catal. B: Environ. 89 (2009) 503–509.
[22] Y. Yu, J.C. Yu, J.G. Yu, Y.C. Kwok, Y.K. Che, J.C. Zhao, L. Ding, W.K. Ge, P.K. Wong, Appl. Catal. A: Gen. 289 (2005) 186–196.
[23] B. Gao, C. Peng, G.Z. Chen, G.L. Puma, Appl. Catal. B: Environ. 85 (2008) 17–23.
[24] D.L. Zhao, X. Yang, C.L. Chen, X.K. Wang, J. Colloid Interface Sci. 398 (2013) 234–239.
[25] H. Liu, H.R. Zhang, H.M. Yang, Chin. J. Catal. 35 (2014) 66–77.
[26] Z. Li, B. Gao, G.Z. Chen, R. Mokaya, S. Sotiropoulos, G.L. Puma, Appl. Catal. B: Environ. 110 (2011) 50–57.
[27] D.X. Hou, R. Goei, X.P. Wang, P.H. Wang, T.T. Lim, Appl. Catal. B: Environ. 126 (2012) 121–133.
[28] S. Muduli, W. Lee, V. Dhas, S. Mujawar, M. Dubey, K. Vijayamohanan, S.H. Han, S. Ogale, ACS Appl. Mater. Interfaces 1 (2009) 2030–2035.
[29] A. Jitianu, T. Cacciaguerra, R. Benoit, S. Delpeux, F. Beguin, S. Bonnamy, Carbon 42 (2004) 1147–1151.
[30] S.H. Wang, S.Q. Zhou, J. Hazard. Mater. 185 (2011) 77–85.
[31] J.Y. Chen, G.Y. Li, Y. Huang, H.M. Zhang, H.J. Zhao, T.C. An, Appl. Catal. B: Environ. 123 (2012) 69–77.
[32] M. Zarei, A. Niaei, D. Salari, A. Khataee, J. Hazard. Mater. 173 (2010) 544–551.
[33] H.L. Liu, Y.R. Chiou, Chem. Eng. J. 112 (2005) 173–179.
[34] A.R. Khataee, M. Fathinia, S. Aber, M. Zarei, J. Hazard. Mater. 181 (2010) 886–897.
[35] A.K. Abdessalem, N. Oturan, N. Bellakhal, M. Dachraoui, M.A. Oturan, Appl. Catal. B: Environ. 78 (2008) 334–341.
[36] Y.J. Xu, Y.B. Zhuang, X.Z. Fu, J. Phys. Chem. C 114 (2010) 2669–2676.
[37] J.Y. Chen, X. Nie, H.X. Shi, G.Y. Li, T.C. An, Chem. Eng. J. 228 (2013) 834–842.
[38] Y. Yu, J.C. Yu, C.Y. Chan, Y.K. Che, J.C. Zhao, L. Ding, W.K. Ge, P.K. Wong, Appl. Catal. B: Environ. 61 (2005) 1–11.
[39] G. Liu, L.Z. Wang, H.G. Yang, H.M. Cheng, G.Q. Lu, J. Mater. Chem. 20 (2010) 831–843.